Faculty and Researchers	Faculty and Researchers Collection

1988

Airborne Surveys of Ocean Current and Temperature Perturbations Induced by Hurricanes

Elsberry, Russell L.; Shay, Lynn K.; Black, Peter G.

Society for Underwater Technology

6

Airborne Surveys of Ocean Current and Temperature Perturbations Induced by Hurricanes

Peter G. Black, National Oceanic and Atmospheric Administration,
Hurricane Research Division, Miami, Florida 33149, USA
and *Russell L. Elsberry* and *Lynn K. Shay,* Department of Meteorology,
Naval Postgraduate School, Monterey, California 93943, USA

As part of a Hurricane Planetary Boundary Layer Experiment, Airborne Expendable Current Profilers (AXCPs) were deployed during the passage of East Pacific Hurricane Norbert and Atlantic Hurricanes Josephine and Gloria on September 23, 1984, October 11, 1984 and September 26, 1985, respectively. The experiment was a joint effort between federal government and private industry which resulted in the first detailed current profile measurements below a hurricane. A total of 92 AXCPs were deployed in these storms, of which 45 transmitted useable data to the NOAA WP-3D aircraft. Most of the failures occurred in the highest wind and wave regions according to Sanford *et al.* (ref. 1). A total of seven satellite-tracked drifting buoys were also deployed in Hurricanes Josephine and Gloria. The Josephine buoys (3) were the Polar Research Lab (PRL) type and were equipped with an anemometer, pressure sensor, and a thermistor chain with sensors at the 40-, 60-, 100- and 200-metre levels. Initial results from analysis of

this data set are provided in Black *et al.* (ref. 2). The Gloria buoys (4) were the Horizon Marine type and were instrumented only for position and sea surface temperature (SST).

The objective of the experiment was to measure the SST decrease induced by these hurricanes together with the storm-generated surface and subsurface current field in order to specify the dynamical processes which are involved. It is hoped that improved parameterizations of the SST decreases and storm-induced currents can be derived from this data set. It has been shown (refs 3 and 4) that the asymmetric SST distributions induced by hurricanes may contribute to their asymmetric structure and reduce air–sea sensible and latent heat fluxes.

The Norbert observations revealed a divergent cyclonic circulation within the mixed layer similar to that predicted by recent numerical model simulations. Maximum mean mixed layer currents of $1.2\,\mathrm{m\,s^{-1}}$ were observed. Below the thermocline, a

weaker anticyclonic circulation was observed, which resulted in 180° phase shifts in current vectors across the thermocline in most quadrants of the hurricane. Local Richardson numbers were less than 0.2 in the right-rear quadrant of Norbert, where sea surface temperature decreases of 2°C were observed in a crescent-shaped pattern centered at a radius 1.5 times the radius of maximum winds. It is uncertain whether these strong currents and large shears are a result of enhanced surface stresses due to fetch-limited seas, as recently proposed by several authors, or to a resonant interaction of the hurricane wind field with inertially rotating currents.

The Josephine and Gloria observations revealed a more complex eddy pattern induced by the interaction of the storm with the ocean Subtropical Front. Maximum inertial current amplitudes of $0.6\,\mathrm{m\,s^{-1}}$ were observed, superimposed on the eddy currents. The Gloria buoy observations were not capable of resolving inertial motions, but did reveal strong, divergent surface currents in the right-rear quadrant, in agreement with the Norbert observations.

Large surface wave-induced currents were observed in the right quadrants of these storms. The largest values of nearly $2\,\mathrm{m\,s^{-1}}$ were observed in Gloria with a period of 12 s. When added to the mean currents of $1\,\mathrm{m\,s^{-1}}$, this resulted in a total peak current of $3\,\mathrm{m\,s^{-1}}$ every 12 s.

RELEVANT AIR–SEA PARAMETERS AND SCALES

The initial upper ocean response, or spin-up, to hurricane forcing is governed by the parameters of the storm. Linear theory of Geisler (ref. 5) has shown that the important parameters for estimating the type of response to be expected are the ratio of the storm translation speed to the first mode internal wave speed (U/C_1) (internal Froude number) and the ratio of the storm forcing scale (scale of positive wind stress curl region) to the baroclinic deformation radius ($2R_m/L_b$, where R_m is the maximum wind radius). The baroclinic radius, L_b, is simply the product of the first mode internal wave speed, C_1, and the inertial period, IP where $IP = 2\pi/24f$, and f is the Coriolis parameter. If the non-dimensional forcing scale is less than one, the response is primarily barotopic. If it is much larger than one, the response is largely baroclinic. If the Froude number is less than $2^{0.5}$, large mean currents are generated and upwelling is the dominant response. If the Froude number is larger than about 5, internal, inertial waves are the dominant type of response. The wavelength of the internal wave response, L_I, is proportional to the product of the baroclinic radius and the Froude number, while the elevation of the resulting baroclinic ridge, ΔH, is proportional to the rate of vorticity input to the ocean, i.e. the wind stress curl. The amplitude of the internal wave response will be small if the non-dimensional time scale, $(2R_m/L_b)/(U/C_1)$, is small compared to $\pi = 3.1416$ according to Veronis (ref. 6) and Geisler and Dickinson (ref. 7).

The observed ocean response parameters for Hurricanes Norbert, Josephine and Gloria are intercompared in Table I. Norbert was a small, intense storm, while Josephine and Gloria were large storms with broad, flat wind profiles. Curiously, all three storms exhibited secondary wind maxima inside of the primary wind maxima. These were remnants of an earlier eyewall, which was contracting and dissipating with time. The evolution of inward propagating convective rings, and their associated wind maxima, is discussed by Willoughby *et al.* (ref. 8). These double wind maxima give rise to considerable difficulty in interpreting the response of a hurricane as a simple Rankin vortex. Does this structure excite a non-linear response or higher harmonics?

One also sees from Table I that Norbert and Josephine were moving slowly with respect to C_1 while Gloria was moving faster. This, together with the fact that the forcing scale ($2R_m$) is of the same order as the baroclinic radius, makes it questionable whether or not linear theory would apply to these

TABLE I

Comparison of ocean response parameters (see text for definitions)

Parameter	Norbert	Josephine	Gloria
R_m, primary (km)	34	52	46
R_{ms}, secondary (km)	17	28	25
τ_m, primary (N m^{-2})	5.7	3.4	3.4
τ_{ms}, secondary (N m^{-2})	4.4	1.4	2.4
curl τ_m, primary ($\times 10^{-3}$)	0.40	0.14	0.02
curl τ_{ms}, secondary ($\times 10^{-3}$)	0.50	0.06	0.10
U (m s^{-1})	3.7	4.2	6.8
C_1 (m s^{-1})	2.8	3.0	3.0
U/C_1	1.4	1.4	2.3
IP (d)	1.6	1.0	1.0
f (s$^{-1} \times 10^4$)	0.50	0.73	0.73
L_b (km)	56	41	41
$2R_m/L_b$	1.1	2.5	2.2
$(2R_m/L_b)/(U/C_1)$	0.8	1.8	1.0
L_I (km)	270	250	515
H (m)	40	55	45
ΔH (m)	12	12	60

cases. A mixed barotropic and baroclinic response is likely. The barotropic response cannot be addressed with AXCP data since these probes measure only relative currents. The combined barotropic and baroclinic response has been recently analysed for another similar case using current meter data by Shay and Elsberry (ref. 9). The baroclinic response for Norbert and Josephine has recently been analysed by Shay et al. (ref. 10), who found that the first four baroclinic modes explained 80 and 60%, respectively, of the current variability. We can also anticipate that the first upwelling peak, displaced one-quarter inertial wavelength ($\frac{1}{4} \times L_I$) behind the storm, would lay just beyond R_m for Norbert and Josephine where wind mixing is anticipated to be a maximum. Thus an interaction between mixing and upwelling would be anticipated for these storms, further complicating the ocean response processes.

MIXED LAYER RESPONSE

A typical SST response pattern with respect to a moving hurricane, shown in Figure 1 as derived by Black (ref. 11), illustrates the crescent-shaped pattern of SST decreases centred at about $2R_m$ to the right-rear of the storm. The SST patterns for Norbert and Josephine are shown in Figures 2 and 3. These fit the pattern of Figure 1 reasonably well with the largest SST decreases being 2.6 and 1.9°C, respectively.
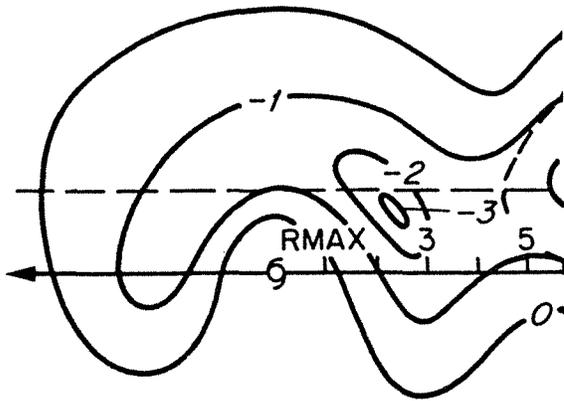

Fig. 1 Schematic SST change in Celsius (°C) induced by a hurricane. The distance scale is indicated in multiples of R_m = RMAX. Storm motion is to the left. Horizontal dashed line is at $1.5R_m$.

The shallowest mixed layer observed in response to Norbert (Fig. 4) occurred about 60 km to the rear of the centre ($\frac{1}{4} \times L_I$), where the mixed layer depth
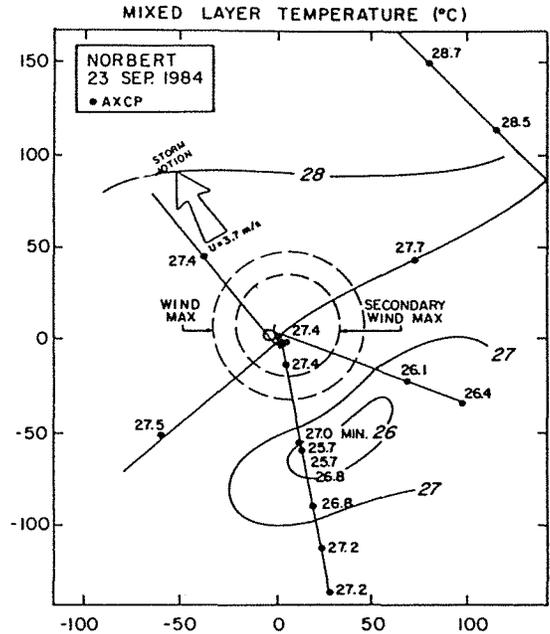

Fig. 2 SST patterns in °C within Hurricane Norbert. Maximum wind radii (primary and secondary) are indicated by quasi-circular dashed lines. Storm motion is indicated by the fat arrow. The SST is shown at AXCP locations (dots) along the aircraft flight path (line).
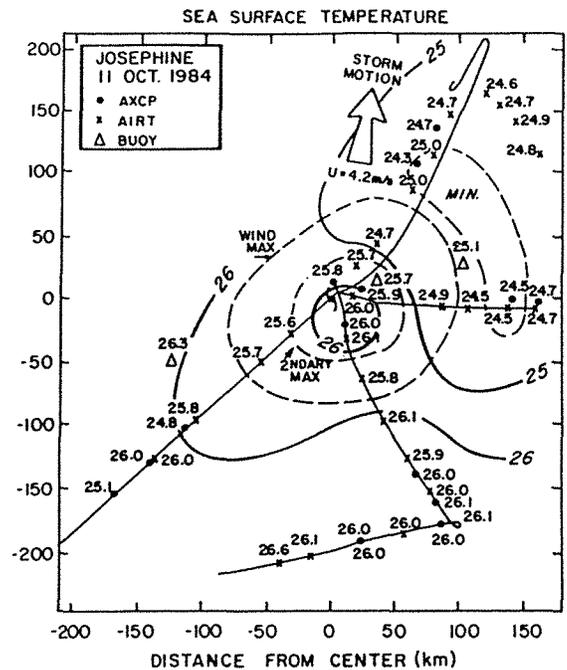

Fig. 3 Same as Fig. 2, except for Hurricane Josephine. Airborne infrared radiation thermometer (AIRT) values of SST are indicated by x.
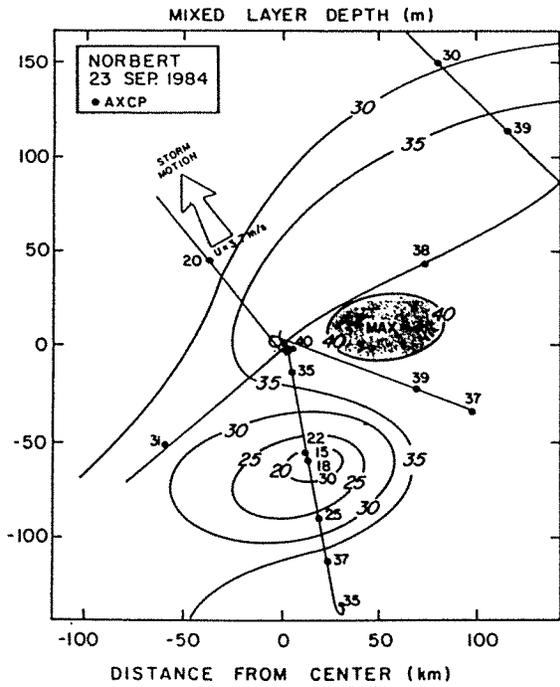
MIXED LAYER DEPTH (m)

Fig. 4 Mixed layer depth (m) within Hurricane Norbert. Maximum depth of greater than 40 m is shaded.
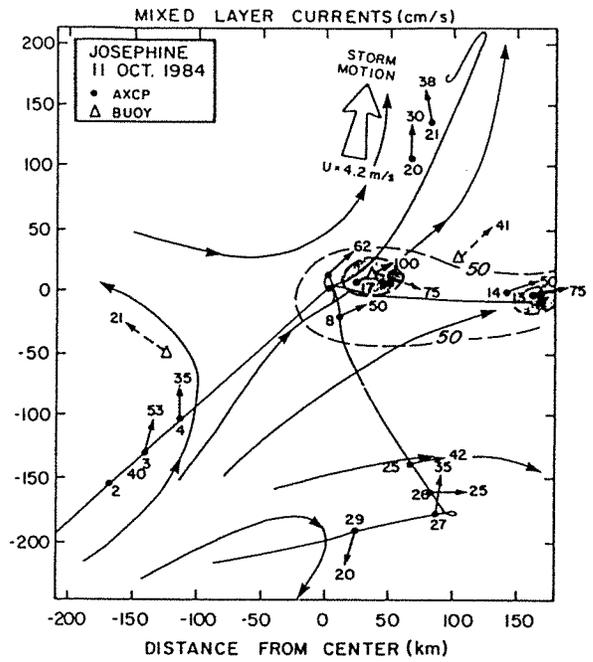
MIXED LAYER CURRENTS (cm/s)

Fig. 6 Same as Fig. 5, except for Hurricane Josephine. Shading indicates currents greater than 75 cm s^{-1}. Open triangles with dashed vectors are buoy motions.
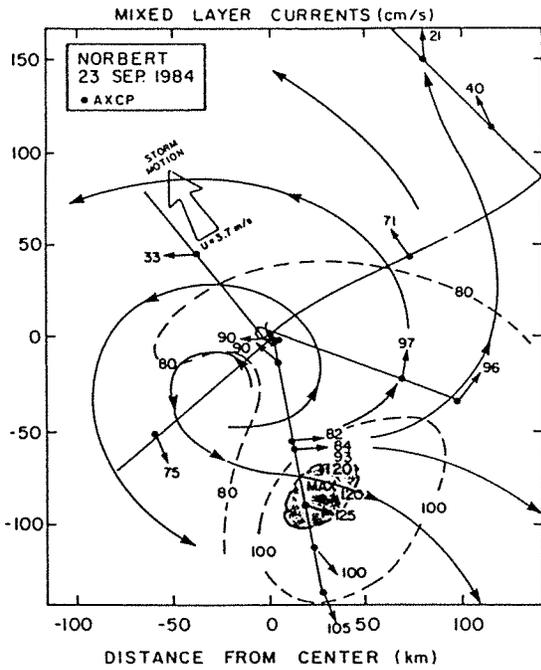
MIXED LAYER CURRENTS (cm/s)

Fig. 5 Streamlines (direction toward) and isotachs of mean mixed layer currents (cm s^{-1}) for Hurricane Norbert. Shading indicates maximum currents of greater than 120 cm s^{-1}.
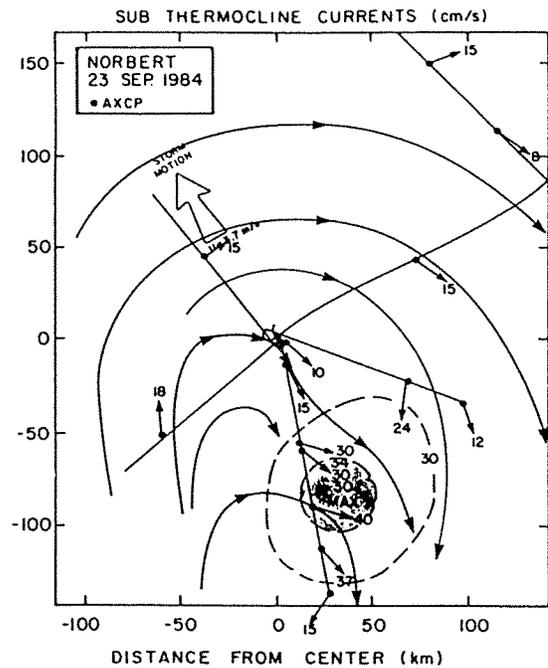
SUB THERMOCLINE CURRENTS (cm/s)

Fig. 7 Sub-thermocline currents (cm s^{-1}) in Hurricane Norbert. Shading indicates currents greater than 40 cm s^{-1}.

(MLD) was only 15 m. The SST minimum in this region appears to be a result of efficiently entrained cooler water from below the shallow mixed layer. Away from this region of strong vertical advection, the mixed layer is deeper (notice the region of greater than 40 m MLD to the right of the storm). The effect of the mixed layer shallowing due to the upwelling is also evident in the mean mixed layer currents (Fig. 5). The Stokes drift associated with large waves (swell) was removed from the AXCP data using the model discussed in Sanford et al. (ref. 1). Maximum mean currents exceed $1\,\mathrm{m\,s^{-1}}$ near $2R_\mathrm{m}$ to the rear of the centre and are directed away from the storm track, which is consistent with the divergent currents associated with inertial pumping. This maximum is superimposed on a general divergent, cyclonic mixed layer current pattern with magnitudes on the order of $80\,\mathrm{cm\,s^{-1}}$, as expected from various numerical models such as in Price (ref. 12). Undoubtedly, larger currents exist at the surface, but could not be measured by AXCPs.

In Hurricane Josephine, the pattern of mixed layer currents is not as well defined due to the presence of the oceanic Subtropical Front (Fig. 6). The maximum currents of 1 m s^{-1} were located just to the right of the storm at about R_m, somewhat closer to the centre than in the case of Norbert. The displacements of the satellite-tracked drifting buoys in Josephine yield a maximum buoy mean speed of 0.5 m s^{-1} according to Black et al. (refs 2 and 13). A recent study by Large et al. (ref. 14) suggests that for the Josephine hull type, the mean mixed layer currents have a weighting factor of 0.5 to 0.6 on the speed of the buoy, giving a mean mixed layer current estimate of 1 m s^{-1}, in agreement with that from the AXCPs. The buoys exhibited widely different trajectories, which is consistent with the highly variable pre-storm currents suggested by Figure 6.

THERMOCLINE RESPONSE

The maximum currents just below the seasonal thermocline (60–160 m) in the rear of Hurricane Norbert were somewhat in excess of 0.4 m s^{-1} (Fig. 7). In this region of strong upwelling, the difference between the sub-thermocline and mixed layer current directions were 40–60°C. However, the sub-thermocline currents in the remainder of the domain were nearly opposite in direction to those in the mixed layer, giving rise to large vertical shears in the thermocline. These shears are shown in Figure 8 together with the bulk and local Richardson numbers (R_i). A substantial area of near critical R_is exist to the right of the storm near the region of the largest SST de-
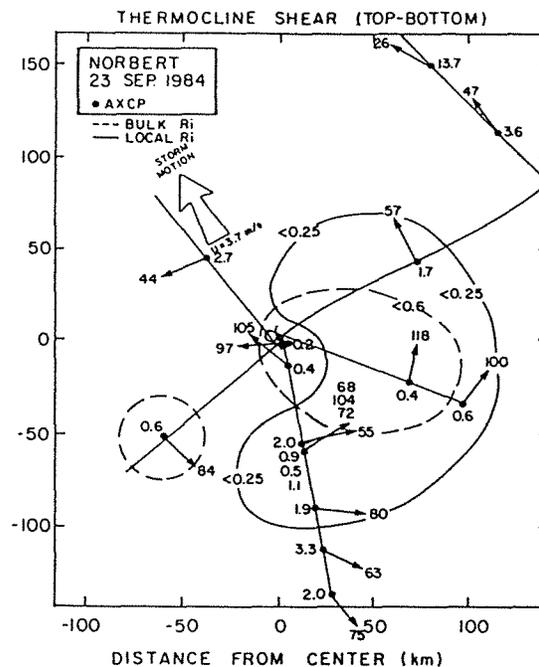

Fig. 8 Thermocline shears (top–bottom) for Hurricane Norbert are indicated near the arrow heads showing the vector shear. Areas exceeding critical bulk and local Richardson numbers (R_i) are outlined in dashed and solid lines, respectively. The local R_i are labelled near the dots.

creases. These direct calculations of R_i are the first confirmation of this physical process that has generally been assumed in numerical models of the oceanic response to hurricanes.

SURFACE WAVE RESPONSE

It is of some interest to examine the wave-induced motions that were subtracted from the AXCP profiles. These wave motions had a period of about 10 s for Norbert and, according to a side-looking airborne radar (SLAR), had a wavelength of 200 m. The wave-induced current is maximum at the surface and decreases exponentially with depth according to e^{-kz}, where $k = 0.0083$ and z is the depth in metres. The maximum surface currents induced by the swell (Fig. 9) were 80 cm s^{-1} and located in the right quadrant of the storm, which is consistent with previous observations showing that highest waves and longest fetches are in the right quadrant. Figure 9 also shows that the pattern of swell propagation is nearly identical to the mean current flow pattern shown in Figure 5. This means that the wave-induced currents are nearly parallel to the mean currents. In the right
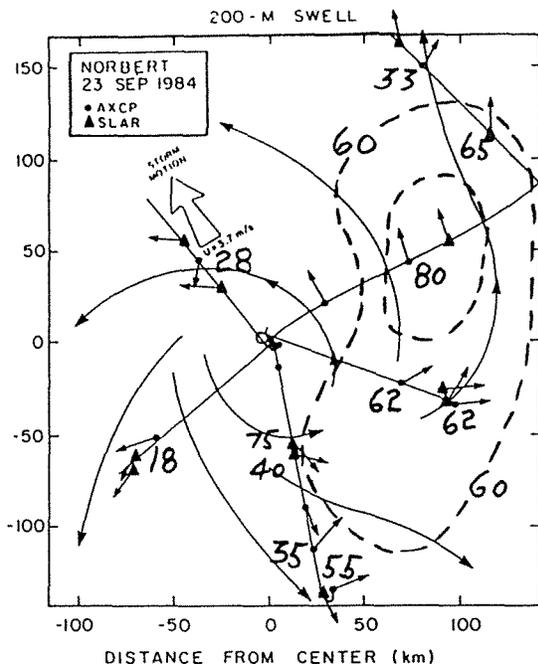
Fig. 9 Streamlines indicating swell propagation direction near Hurricane Norbert. Surface, wave-induced Stokes drift velocity (cm s^{-1}) is contoured with a dashed line. Triangles indicate swell directions obtained from side-looking airborne radar (SLAR) images.

quadrant, the mean current is modulated by 110% at the surface with a 10 s period. The total current thus varies from zero to 1.5 m s^{-1}. In the rear quadrant, there is only a 25% modulation, resulting in a maximum total current of about 1.7 m s^{-1}. It is conceivable that this wave-induced motion may also modulate the shear at the base of the mixed layer, producing intermittent mixing with a 10 s period, and playing an important role in the mixing processes.

HURRICANE GLORIA RESULTS

During the AXCP deployment in Hurricane Gloria, four Horizon Marine mini-drifting buoys were deployed in the storm along a line extending from the radius of maximum wind to a point 190 km northeast of the centre. The buoys contained the Service ARGOS transmitters for communicating the buoy's position and sea surface temperature data via NOAA polar orbiting satellites. The buoys were launched from the NOAA WP-3D research aircraft via the internal launch chute, which was the first such deployment of its kind. The buoys were deployed from an

altitude of 3 km and fell freely to the surface, where a drogue was deployed from each, descending to a depth of 25 m. Fortuitously, a fifth drifting buoy deployed 9 months earlier by oceanographers from NOAA was also in the area traversed by Gloria.

The primary purpose for deploying the buoys in Gloria was to map the background circulation features present in the region in order to place the AXCP measurements in proper perspective with respect to the prevailing currents. The second objective in deploying the buoys was to provide independent confirmation of surface mean currents in the vicinity of the hurricane for comparison with AXCP derived mean surface currents.

The buoy trajectories for the first 12 days after hurricane passage (Fig. 10) reveal the location of anticyclonic and cyclonic eddy centres indicated by an 'A' and 'C', respectively, and hence substantiate the existence of fairly energetic eddy currents in the semi-permanent Subtropical Front first described by Voorhis (ref. 15). The anticyclonic centre northeast of the storm track most likely existed prior to the passage of the storm. However, it is unclear whether the cyclonic centre along the storm track was induced by the storm or whether it existed prior to storm passage.
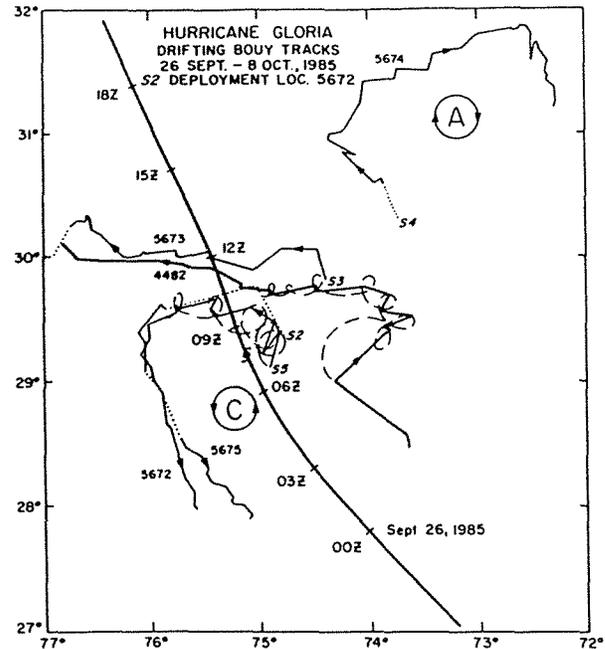

Fig. 10 Mini-buoy trajectories for a two-week period following the passage of Hurricane Gloria. Anticyclonic (A) and cyclonic (C) eddy centres are indicated, as are storm 3-hourly positions and track.

The AOML buoy was undrogued and hence exhibited the largest deflection to the right of the track by the storm-induced currents. An average buoy velocity over the 12 hours between fixes of $1.4 \, \text{m s}^{-1}$ was calculated during the time of the rightward deflection. This is probably representative of true mixed layer currents since drag on the mini-buoy was much smaller than drag on the larger PRL drifting buoys used in Josephine. However, instantaneous velocities, associated with hypothesized inertial period currents (dashed lines), were probably somewhat higher.

Figure 11 illustrates the average mixed layer current field derived from the AXCP data. Also indicated on Figure 11 by triangles are the current vectors derived from the drifting buoys which agree, to within $10 \, \text{cm s}^{-1}$, with the AXCP currents. Note that the location of the cyclonic centre of circulation (strongly divergent and indicative of upwelling), corresponds to the cyclonic eddy centre inferred from the buoys. Both the buoys and the AXCPs indicate that the strongest currents are located in the right rear quadrant of the storm, in agreement with the findings from Norbert. In the Gloria case, the mean current

speeds are somewhat larger than Norbert, peaking at $1.85 \, \text{m s}^{-1}$.

The wave-induced motions at the surface were also larger in Gloria than in Norbert, with amplitudes of 1.5 to $2.0 \, \text{m s}^{-1}$ and periods of $12 \, \text{s}$ in the right-front quadrant. This modulated the mean currents in this region by 200%. Maximum total currents in this region thus approached $3 \, \text{m s}^{-1}$.

In conclusion, it can be said that the concurrent use of drifting buoys to provide a time history and AXCPs to provide a spacial snapshot greatly enhances the data base for a hurricane–ocean response experiment. Buoys with surface meteorological sensors, although more expensive, also aid in defining the surface wind field which forces the ocean response. It is highly recommended that the two tools—AXCPs and mini-drifting buoys—be used together in future experiments.

CONCLUSIONS

As shown above, the ocean response to a hurricane is primarily governed by the parameters of the forcing (Table I). The most crucial parameters seem to be the storm's translational motion and its maximum wind radius. The ocean dynamics can also be quite complicated, especially in areas of pre-existing ocean eddies, such as the Subtropical Front. Future ocean response experiments should be conducted away from these features to simplify the interpretation of the data.

Such features as secondary wind maxima (associated with 'double eye' features on radar displays of precipitation), exhibited by all three storms in this study, have not been treated in ocean response models. Such secondary maxima may introduce other scales into the problem than predicted by linear theory. Future experiments should accurately measure these mesoscale features so that their impact on the ocean currents and associated SST changes can be assessed and models to predict them correctly formulated.

It appears that storms with the right combination of storm speed, size and/or secondary wind maxima which generate upwelling just beyond the radius of maximum wind create conditions favourable for rapid and large decrease in SST. With this condition shown to be a maximum in the right-rear quadrant, where inflowing air from outside the storm must pass, considerable modification of inflowing air to the storm can take place as well as modification of vertical air–sea fluxes, both of which can lead to a modification of the storm intensification rate.
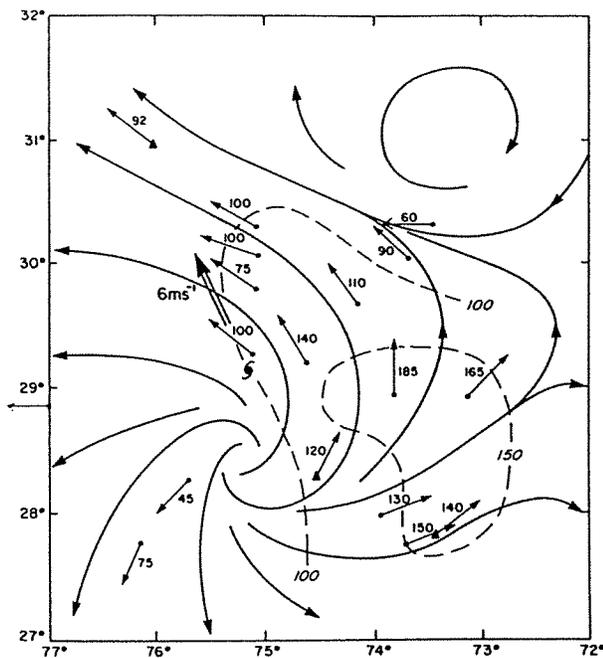

Fig. 11 Same as Fig. 5, except for Hurricane Gloria. AXCP positions are indicated by dots with current vector and magnitude shown. Triangles indicate mini-buoy locations and the arrow is their motion vector.

REFERENCES

1. Sanford, T. B., Black, P. G., Haustein, J., Feeney, J. W., Forristall, G. Z. and Price, J. F. (in press). Ocean response to hurricanes, Part I: Observations. *J. Geophys. Res.* Gill Memorial Issue.
2. Black, P. G., Elsberry, R. L., Shay, L. K., Partridge, R. and Hawkins, J. (in press). Hurricane Josephine surface winds and ocean response determined from air-deployed drifting buoys and concurrent research aircraft data. *J. Oceanic Atm. Tech.*
3. Holland, G. J. and Black, P. G. (in press). The boundary layer of Hurricane Kerry (1979), I: Mesoscale Structure. Submitted to *J. Atm. Sci.*
4. Black, P. G., Holland, G. J. and Powell, M. D. (in press). The boundary layer of Hurricane Kerry (1979), II: heat and moisture budgets. Submitted to *J. Atm. Sci.*
5. Geisler, J. E. (1970). Linear theory on the response of a two layer ocean to a moving hurricane. *Geophys. Fluid Dyn.* **1**: 249–272.
6. Veronis, G. (1956). Partition of energy between geostrophic and nongeostrophic oceanic motions. *Deep Sea Res.* **3**: 157–177.
7. Geisler, J. E. and Dickinson, R. E. (1972). The role of variable Coriolis parameter in the propagation of inertia-gravity waves during the process of geostrophic adjustment. *J. Phys. Oceanogr.* **2**: 263–272.
8. Willoughby, H. E., Marks, F. D. Jr. and Feinberg, R. W. (1984). Stationary and moving convective bands in hurricanes. *J. Atm. Sci.* **41**: 3189–3211.
9. Shay, L. K. and Elsberry, R. L. (1987). Near-inertial ocean current response to Hurricane Frederic. *J. Phys. Oceanogr.* **17**: 1249–1269.
10. Shay, L. K., Elsberry, R. L. and Black, P. G. (in preparation). Near-inertial ocean current response to Hurricanes Norbert and Josephine.
11. Black, P. G. (1983). Ocean Temperature Changes Induced by Tropical Cyclones. PhD dissertation, the Pennsylvania State University, University Park, PA, 278 pp.
12. Price, J. F. (1981). Upper ocean response to a hurricane. *J. Phys. Oceanogr.* **11**: 153–175.
13. Black, P. G., Elsberry, R. L., Shay, L. K. and Partridge, R. (1985). Hurricane Josephine surface winds and ocean response determined from air-deployed drifting buoys and concurrent research aircraft data. Extended Abstracts, 16th Conf. Hurr. and Trop. Met., Amer. Met. Soc., Boston, MA, pp. 22–24.
14. Large, W. G., McWilliams, J. C. and Niiler, P. P. (1986). Upper ocean thermal response to strong autumnal forcing of the Northeast Pacific. *J. Phys. Oceanogr.* **16**: 1524–1550.
15. Voorhis, A. D. (1969). The horizontal structure of thermal fronts in the Sargasso Sea. *Deep Sea Res.* **16** (Suppl), 331–337.